doi:10.1093/brain/aws343 Brain 2013: 136; 926–943 | 926

BRAIN
A JOURNAL OF NEUROLOGY

Co-induction of the heat shock response ameliorates disease progression in a mouse model of human spinal and bulbar muscular atrophy: implications for therapy

Bilal Malik,[1,2,*] Niranjanan Nirmalananthan,[1,2,*] Anna L. Gray,[1,2] Albert R. La Spada,[3,4] Michael G. Hanna[2,5] and Linda Greensmith[1,2]

1 Sobell Department of Motor Neuroscience and Movement Disorders, UCL Institute of Neurology, Queen Square, London, WC1N 3BG, UK
2 MRC Centre for Neuromuscular Diseases, UCL Institute of Neurology, Queen Square, London, WC1N 3BG, UK
3 Division of Genetics, Department of Paediatrics, Department of Cellular and Molecular Medicine, the Institute for Genomic Medicine, and the Sanford Consortium for Regenerative Medicine, University of California San Diego, La Jolla, CA 92037, USA
4 Rady Children's Hospital, San Diego, CA 92123, USA
5 Department of Molecular Neuroscience, UCL Institute of Neurology, Queen Square, London, WC1N 3BG, UK

*These authors contributed equally to this work.

Correspondence to: Linda Greensmith,
Sobell Department of Motor Neuroscience,
MRC Centre for Neuromuscular Diseases,
UCL Institute of Neurology,
Queen Square, London, WC1N 3BG, UK
E-mail: l.greensmith@ucl.ac.uk

Spinal and bulbar muscular atrophy, also known as Kennedy's disease, is an adult-onset hereditary neurodegenerative disorder caused by an expansion of the polyglutamine repeat in the first exon in the androgen receptor gene. Pathologically, the disease is defined by selective loss of spinal and bulbar motor neurons causing bulbar, facial and limb weakness. Although the precise disease pathophysiology is largely unknown, it appears to be related to abnormal accumulation of the pathogenic androgen receptor protein within the nucleus, leading to disruption of cellular processes. Using a mouse model of spinal and bulbar muscular atrophy that exhibits many of the characteristic features of the human disease, *in vivo* physiological assessment of muscle function revealed that mice with the pathogenic expansion of the androgen receptor develop a motor deficit characterized by a reduction in muscle force, abnormal muscle contractile characteristics, loss of functional motor units and motor neuron degeneration. We have previously shown that treatment with arimoclomol, a co-inducer of the heat shock stress response, delays disease progression in the mutant superoxide dismutase 1 mouse model of amyotrophic lateral sclerosis, a fatal motor neuron disease. We therefore evaluated the therapeutic potential of arimoclomol in mice with spinal and bulbar muscular atrophy. Arimoclomol was administered orally, in drinking water, from symptom onset and the effects established at 18 months of age, a late stage of disease. Arimoclomol significantly improved hindlimb muscle force and contractile characteristics, rescued motor units and, importantly, improved motor neuron survival and upregulated the expression of the vascular endothelial growth factor which possess neurotrophic activity. These results provide evidence that upregulation of the heat shock response by treatment with arimoclomol may have therapeutic potential in the treatment of spinal and bulbar muscular atrophy and may also be a possible approach for the treatment of other neurodegenerative diseases.

Received May 15, 2012. Revised October 30, 2012. Accepted November 6, 2012. Advance Access publication February 7, 2013
© The Author (2013). Published by Oxford University Press on behalf of the Guarantors of Brain. All rights reserved.
For Permissions, please email: journals.permissions@oup.com

Keywords: polyglutamine expansions; motor neuron disease; heat shock protein; protein aggregation; neuroprotective agents

Abbreviations: AR20 = androgen receptor with 20 polyglutamine repeats; AR100 = androgen receptor with 100 polyglutamine repeats; HSF1 = heat shock factor 1; Hsp = heat shock protein; SOD1 = superoxide dismutase 1 enzyme

Introduction

Spinal and bulbar muscular atrophy, otherwise known as Kennedy's disease, is an X-linked, late-onset progressive neuromuscular disease that predominantly affects males. Clinically, the disease is characterized by atrophy, fasciculation and weakness of the facial, bulbar and proximal limb muscles, together with mild sensory impairment and manifestations of androgen insensitivity (Chahin *et al*., 2008; Suzuki *et al*., 2008; Banno *et al*., 2009; Rhodes *et al*., 2009). Molecularly, the disease results from an expansion in the glutamine repeat tract in the androgen receptor (*AR*) gene which encodes a polyglutamine tract in the translated protein (La Spada *et al*., 1991; Fischbeck, 2001). The polymorphic trinucleotide CAG repeat normally ranges from 9 to 36, but an expansion of >38 repeats results in disease (La Spada *et al*., 1991). Although the expanded androgen receptor protein is ubiquitously expressed, the precise mechanistic basis for the selective death of bulbar and lower motor neurons remains unknown. Spinal and bulbar muscular atrophy belongs to a family of nine polyglutamine repeat expansion diseases including Huntington's disease, dentatorubral pallidoluysian atrophy and six spinocerebellar ataxias, which share many common features and underlying pathological mechanisms (Ross, 2002; Gatchel and Zoghbi, 2005). Several mechanisms, acting either independently or as a part of a more complex pathway, have been suggested to play a role in the pathogenesis of spinal and bulbar muscular atrophy. Considerable evidence now indicates a role for ligand-dependent translocation into the nucleus (Takeyama *et al*., 2002; Walcott and Merry, 2002) and nuclear accumulation of the pathogenic protein (Adachi *et al*., 2005), misfolding of the expanded protein (Stenoien *et al*., 1999; Li *et al*., 2007; Rusmini *et al*., 2011), impaired clearance of the androgen receptor protein (Montie *et al*., 2009) and transcriptional dysregulation (Sopher *et al*., 2004; Katsuno *et al*., 2006, 2010*a*). Importantly, no effective treatment that has acceptable side effects is currently available to counteract the pathology or control the progression of symptoms in spinal and bulbar muscular atrophy.

The androgen receptor is a steroid hormone receptor that is restricted to the cytoplasm in a complex with the heat shock proteins Hsp90 and Hsp70. Binding of the ligand permits dissociation from this complex, allowing translocation of the androgen receptor to the nucleus, resulting in activation of target genes (Heinlein and Chang, 2001). However, pathogenic expansion of the polyglutamine repeat tract in androgen receptor and other polyglutamine proteins may result in a conformational change in the aberrant protein, facilitating its aggregation into inclusions (Perutz *et al*., 1994; Williams and Paulson, 2008). In spinal and bulbar muscular atrophy, although the polyglutamine-expanded androgen receptor accumulates into nuclear and cytoplasmic inclusions in both neural and non-neural tissues, the disease is primarily characterized by the presence of nuclear inclusions of aggregated protein within motor neurons (Adachi *et al*., 2005). These inclusion bodies harbour components of the ubiquitin–proteasome system (NEDD8, an ubiquitin-like protein; and PA700, the 26S proteasome cap), protein chaperones including heat shock proteins (Hdj2, Hsc70, Hsp70 and Hsp90), and several transcriptional factor co-activators (the steroid receptor coactivator 1, SRC-1, now known as NCOA1; and CREB-binding protein, CREBBP) (Stenoien *et al*., 1999; Abel *et al*., 2001; Adachi *et al*., 2001). However, the precise nature of the inclusions remains contentious, with little direct relationship between the presence of aggregates and cell death (Simeoni *et al*., 2000; Taylor *et al*., 2003; Takahashi *et al*., 2008). Indeed there is a greater frequency of occurrence of diffuse nuclear accumulation of the expanded androgen receptor that correlates with the CAG repeat length (Adachi *et al*., 2005). Nevertheless, nuclear aggregates are a hallmark of the disease, which arise through adoption of an abnormal protein conformation favouring aggregation (Perutz *et al*., 1994; Williams and Paulson, 2008). Furthermore, the presence within these inclusions of proteins involved in refolding and the chaperone pathway, suggest an association of these mechanisms with pathology, even though inclusions themselves may not represent the primary or earliest toxic species in polyglutamine repeat expansion disease (Yoo *et al*., 2003; Arrasate *et al*., 2004; Bowman *et al*., 2005; Li *et al*., 2007; Hands and Wyttenbach, 2010). In addition, it has been reported that the formation of nuclear micro-aggregates that are not microscopically visible, but derived from soluble oligomeric forms of the pathogenic proteins, may in fact represent the primary and earliest focus of pathology (Li *et al*., 2007; Takahashi *et al*., 2008). The presence of oligomers may enhance and lead to the formation of micro-aggregates, not normally detected with conventional microscopic techniques, but which nevertheless will be detrimental to motor neurons (Ross and Poirier, 2005; Williams and Paulson, 2008).

Several treatment strategies for spinal and bulbar muscular atrophy have therefore focused on decreasing nuclear accumulation, diminishing protein misfolding and augmenting the clearance of the expanded androgen receptor by either genetic or pharmacologically induced overexpression of heat shock proteins (Bailey *et al*., 2002; Waza *et al*., 2005; Adachi *et al*., 2007; Tokui *et al*., 2009). In an AR-97Q spinal and bulbar muscular atrophy mouse model, treatment with Hsp90 inhibitors and inducers of heat shock proteins, which may enhance the removal of misfolded protein, has been shown to improve the neuromuscular phenotype of these mice (Waza *et al*., 2005; Tokui *et al*., 2009). However, the anti-cancer agents used in these studies may be associated with significant adverse effects (Banerji *et al*., 2005). We have previously used an alternative approach to upregulate the expression of heat shock proteins in the mutant superoxide dismutase 1 enzyme (SOD1) mouse model of amyotrophic lateral sclerosis, an aggressive and usually fatal adult motor neuron disorder. Treatment of SOD1 mice with arimoclomol, a novel co-inducer

of the heat shock response, was successful in ameliorating pathology and extending lifespan of SOD1 mice, even when administered after symptom onset (Kieran *et al*., 2004; Kalmar *et al*., 2008). Arimoclomol is currently in clinical trials in patients with amyotrophic lateral sclerosis in the USA (Cudkowicz *et al*., 2008; Lanka *et al*., 2009). An important characteristic of arimoclomol is that it selectively targets cells undergoing a stress response, thereby acting as a co-inducer rather than an inducer of the heat shock response, resulting in significantly fewer of the side effects associated with direct activation of the heat shock response (Kieran *et al*., 2004; Kalmar *et al*., 2008). Arimoclomol has been shown to prolong the activation of heat shock transcription factor 1 (HSF1) (Hargitai *et al*., 2003), and thereby upregulate heat shock protein expression both *in vitro* (Vigh *et al*., 1997; Kalmar *et al*., 2008) and *in vivo* (Kieran *et al*., 2004; Kalmar *et al*., 2008), effects that are likely to facilitate the refolding and removal of non-native toxic proteins. Therefore, in this study we examined whether arimoclomol may provide an effective and safe therapy for spinal and bulbar muscular atrophy. Using the AR100 mouse model of spinal and bulbar muscular atrophy which recapitulates the course and pathology of disease observed in humans (Sopher *et al*., 2004; Chahin *et al*., 2008; Malik *et al*., 2011), we tested the ability of arimoclomol to ameliorate disease progression. In these mice, the expanded androgen receptor is expressed at endogenous levels and importantly, male mice carrying the expanded androgen receptor with 100 polyglutamine repeats (pathogenic AR100 mice) develop significant motor neuron degeneration, leading to a progressive late-onset neuromuscular phenotype (Sopher *et al*., 2004; Chahin *et al*., 2008; Malik *et al*., 2011). Control mice expressing the androgen receptor with 20 polyglutamine repeats (non-pathogenic AR20 mice) do not manifest any phenotype, as <38 polyglutamine repeats in humans are not linked with spinal and bulbar muscular atrophy (La Spada *et al*., 1991; Gatchel and Zoghbi, 2005).

Our results show that treatment with arimoclomol from the time of symptom onset dramatically delayed progression of the neuromuscular phenotype in AR100 spinal and bulbar muscular atrophy mice. In particular, our findings reveal the neuroprotective effects of arimoclomol in enhancing the survival of motor neurons, the loss of which is fundamental in the development of spinal and bulbar muscular atrophy (Fischbeck, 1997; Sopher *et al*., 2004; Adachi *et al*., 2005; Malik *et al*., 2011), may well be mediated by upregulation of the neurotrophic factor, vascular endothelial growth factor.

Materials and methods

Breeding and maintenance of mutant androgen receptor spinal and bulbar muscular atrophy mice

All experimental procedures were carried out under licence from the UK Home Office (Scientific Procedures Act 1986), and following approval by the Ethical Review Panel of UCL Institute of Neurology. Yeast artificial chromosome mice containing the mutant human androgen receptor transgene, expressed at endogenous levels and described previously (Sopher *et al*., 2004; Thomas *et al*., 2006; Malik *et al*., 2011), were bred and maintained at UCL Institute of Neurology Biological Services. Heterozygote males carrying the androgen receptor with 100 polyglutamine repeats (pathogenic AR100 mice) or 20 polyglutamine repeats (non-pathogenic AR20 mice) were mated with wild-type C57BL/6J females. In keeping with the gender specificity of the disease, only male offspring showed a disease phenotype and so only male mice were used in this study. The mice were genotyped by PCR amplification of ear notches using a forward (5′-catctgagtccaggggaacagc-3′) and reverse primer (5′-gcccag gcgctgccgtagtcc-3′). PCR products were digested with BglI (New England Biolabs) and analysed using agarose gel electrophoresis and visualized using GelRed™ stain (Sigma-Aldrich). In addition, in some experiments, male age-matched wild-type littermates were also used as controls.

Treatment of mice with arimoclomol

Following genotyping, male mice were randomly assigned to a treatment or vehicle arm of the study. From 12 months of age to the time of examination at 18 months, male AR100 mice were treated with either 120 mg/kg/day arimoclomol dissolved in drinking water ($n = 10$) or water alone (vehicle; $n = 10$). The body weight of arimoclomol and vehicle-treated AR100 mice was recorded monthly. All mice used in this study were littermates and were housed in a controlled temperature and humidity environment with a 12-h light/dark cycle and had access to drinking water and food *ad libitum*. To examine the induction of heat shock proteins, arimoclomol was given by daily intraperitoneal injection at a dose of 120 mg/kg for a period of 16 days, while control mice received vehicle (saline).

Western blot

Western blot was performed to determine protein levels as described (Malik *et al*., 2008*a*, *b*). Briefly, proteins were separated by SDS-PAGE, transferred onto nitrocellulose membrane, incubated with indicated primary antibodies (Hsp70, Stressgen; Hsp90, Santa Cruz; β-actin, Abcam; α-tubulin DM1A, Sigma) followed by either anti-mouse Alexa Fluor® 680 (Invitrogen) or anti-rabbit IRDye800® (Rocklard) secondary antibodies. Blots were analysed using the Odyssey detection system (Licor), and densitometry was performed using the Odyssey software.

Real-time quantitative polymerase chain reaction

Total RNA was extracted from tissue using the guanidine isothiocyanate-based method (Chomczynski and Sacchi, 1987) using TRIzol® solution (Invitrogen) according to the manufacturer's instructions. Complementary DNA was prepared using 1 μg total RNA primed with oligo(dT) and SuperScript® III reverse transcriptase, according to the protocol supplied by the manufacturer (Invitrogen). Real-time quantitative PCR was performed as described (Malik *et al*., 2012), using SYBR® Green PCR master mix (Applied Biosystems), template- and gene-specific primers in a total volume of 20 μl. After an initial denaturation at 95°C for 10 min, templates were amplified by 40 cycles of 95°C for 15 s and 60°C for 1 min in an Applied Biosystems 7500 Real-Time PCR System. A dissociation curve was generated to ensure there was amplification of a single product and absence of primer dimers. Reactions were performed in triplicate, and

gene expression values were normalized using the geometric mean of the housekeeping genes, β-actin and hypoxanthine guanine phosphoribosyl transferase 1 (*Hprt1*) (Vandesompele *et al*., 2002). Gene expression was calculated by the comparative threshold cycle (ddCt) method (Livak and Schmittgen, 2001), and an unpaired *t*-test was used to determine statistical significance.

Physiological assessment of muscle function and motor unit survival

The primary characteristic phenotype of spinal and bulbar muscular atrophy is a loss of muscle function as a result of motor neuron degeneration. The neuromuscular phenotype of heterozygote AR100 male mice, which either carry the pathogenic androgen receptor (AR100 mice) or non-pathogenic androgen receptor transgene (AR20), was therefore characterized at a late stage of disease, when the mice were 18 months old, and compared with age-matched male wild-type littermates. In the experiments to investigate the effects of arimoclomol, AR100 mice treated with arimoclomol or vehicle were also examined at 18 months. In addition, mice homozygote for AR100 were examined at 13 months of age when they showed a similar disease phenotype to that observed in 18-month heterozygote AR100 mice.

The mice were prepared for *in vivo* assessment of muscle function as previously described (Kieran *et al*., 2004; Bilsland *et al*., 2006; Kalmar *et al*., 2008). The mice were deeply anaesthetized using isoflurane inhalation delivered through a Fortec vaporizer (Vet Tech Solutions Ltd) by placing the animals in an induction chamber containing 1.5–2.0% isoflurane in oxygen. Anaesthesia was maintained with the same mixture delivered through a facemask and adjusted to maintain depth of anaesthesia. The distal tendons of the tibialis anterior and extensor digitorum longus muscles in both hindlimbs were dissected free and attached to isometric force transducers (Dynamometer UFI Devices). The sciatic nerve was exposed, sectioned and all branches cut except for the deep peroneal nerve that innervates the tibialis anterior and extensor digitorum longus muscles. Experiments were carried out at room temperature, with the length of the muscles adjusted for maximum twitch tension and the muscles and nerves kept moist with saline throughout the recordings. Isometric contractions were elicited by stimulating the nerve to extensor digitorum longus and tibialis anterior muscles using square-wave pulses of 0.02 ms duration at supra-maximal intensity using silver wire electrodes. Contractions were elicited by trains of stimuli at frequencies of 40, 80 and 100 Hz for 450 ms and the maximum twitch and tetanic tension was measured using the force transducers, which were connected to a Picoscope 3423 oscilloscope (Pico Technology) and analysed using Picoscope Software v5.16.2 (PicoTechnology).

Following recording of isometric tension, the contractile and fatigue characteristics of extensor digitorum longus muscles were determined. The time to peak contraction was calculated by measuring the time taken (ms) for the muscles to elicit peak twitch tension and the half relaxation time (the time taken for the muscles to reach half relaxation from peak contraction) was also calculated.

The number of motor units innervating the extensor digitorum longus muscles in both hindlimbs was determined by stimulating the motor nerve with stimuli of increasing intensity, resulting in stepwise increments in twitch tension due to successive recruitment of motor axons. The number of stepwise increments was counted to give an estimate of the number of motor units present in each extensor digitorum longus muscle.

In addition, the resistance of the extensor digitorum longus muscles to fatigue was assessed by repeated stimulation at 40 Hz for 250 ms/s for 3 min. The tetanic contractions were recorded on a Lectromed Multitrace 2 recorder (Lectromed Ltd). The decrease in tension after 3 min of stimulation was measured and a fatigue index was calculated, with a fatigue index approaching a value of 1.0 indicating that a muscle is highly fatigable (Sharp *et al*., 2005).

Motor neuron survival

Following removal of the muscles, the mice were perfused and the lumbar spinal cord was removed for determination of motor neuron survival, as previously described (Kieran *et al*., 2004; Malik *et al*., 2011). The mice were terminally anaesthetized with pentobarbitone, transcardially perfused with 4% paraformaldehyde and the lumbar region of the spinal cord was removed. Serial 20-μm transverse sections were cut on a cryostat, stained with gallocyanin (a Nissl stain) and the number of positively stained motor neurons in the sciatic motor pool of every third section between the L2 and L5 levels of the spinal cord was counted, as previously described (Kieran *et al*., 2004; Malik *et al*., 2011). Only large polygonal neurons with a clearly identifiable nucleus and nucleolus were included in counts. This protocol avoids the possibility of counting the same cells twice in consecutive sections.

Statistical analysis

Statistical analysis was performed using SPSS v15 (SPSS Inc), with the Mann–Whitney U test, Kruskal–Wallis or one-way ANOVA with *post hoc* analysis to evaluate significance of data. A *P*-value of <0.05 was considered statistically significant.

Results

The expression levels of heat shock proteins in spinal and bulbar muscular atrophy mice

We first set out to examine the expression of several cytoprotective heat shock proteins in the AR100 mouse model of spinal and bulbar muscular atrophy, as levels of these proteins have been reported to be reduced in mouse models of polyglutamine repeat expansion diseases, including spinal and bulbar muscular atrophy (Adachi, 2003; Katsuno, 2005; Labbadia *et al*., 2011). The expression levels of the stress-induced form of Hsp70, as well as Hsp90, were examined in the spinal cord of presymptomatic (Fig. 1A), symptomatic (Fig. 1B) and mice late in the disease stage (Fig. 1C). Presymptomatic mice displayed a slight decrease in the levels of Hsp70 in AR100 spinal and bulbar muscular atrophy mice compared with wild-type, although this did not reach significance (Fig. 1A). Interestingly, in symptomatic mice the Hsp70 expression levels increased again and were comparable with wild-type (Fig. 1B), perhaps as a reflection of the induced stress of the onset of disease. By late stage, Hsp70 was significantly reduced in AR100 mice (Fig. 1C). No change in Hsp90 was observed at any age.

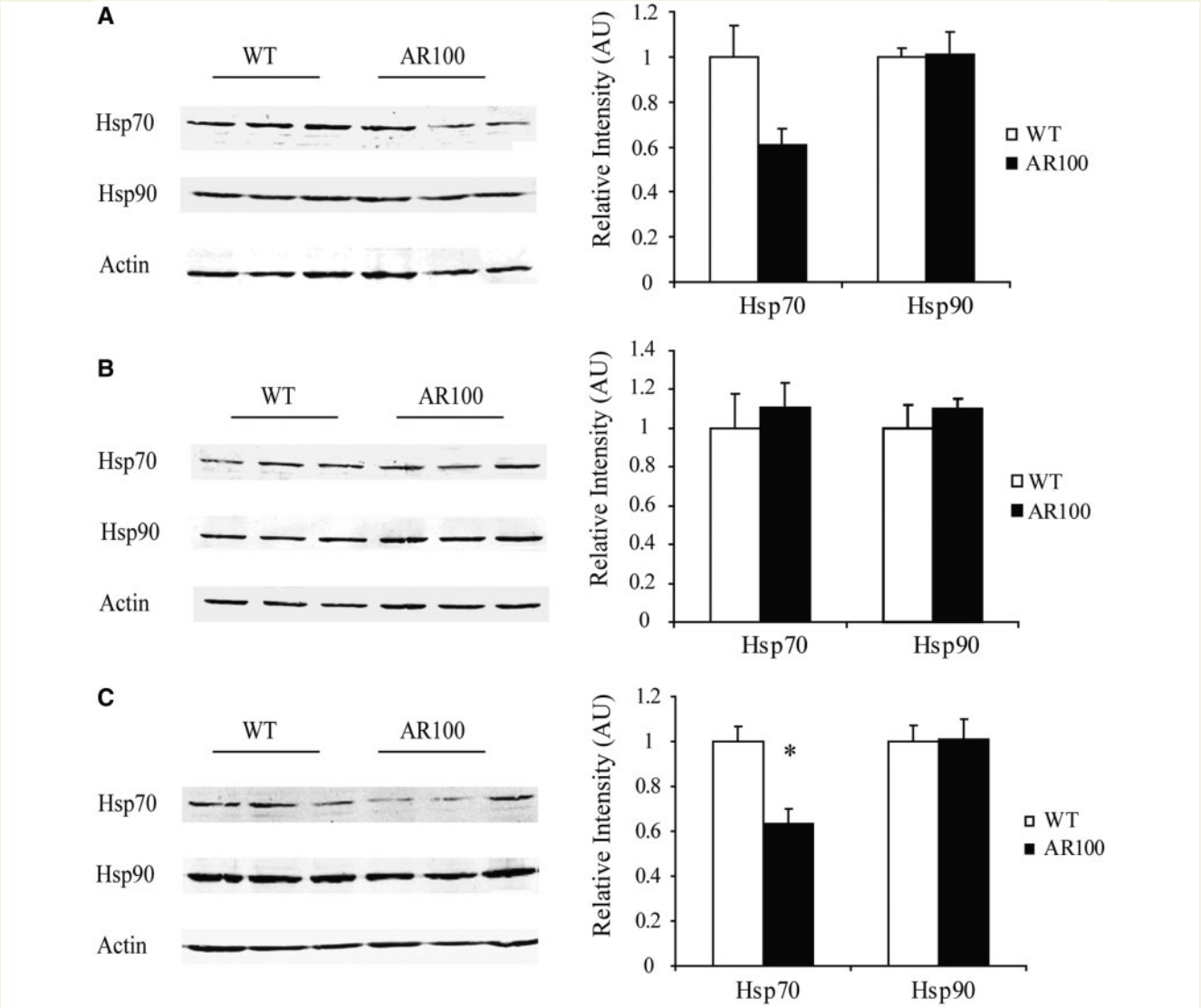

Figure 1 Examination of expression levels of heat shock proteins in mice with spinal and bulbar muscular atrophy. The expression levels of Hsp70 and Hsp90 were analysed in spinal cord of (**A**) presymptomatic (3 month), (**B**) symptomatic (12 month) and (**C**) late stage (18 month) wild-type (WT) and AR100 mice. Densitometric analysis of bands was performed using values normalized to actin. Data are displayed as mean ± SEM and are representative of three independent experiments. Statistical analysis was performed using a two sample *t*-test ($n \geqslant 3$, $^*P < 0.05$). AU = arbitrary units.

Arimoclomol upregulates Hsp70 in the spinal cord and hindlimb muscles of spinal and bulbar muscular atrophy mice

We have previously shown that treatment with arimoclomol, a novel heat shock protein co-inducer, delays disease progression and improves the neuromuscular deficit in a mutant SOD1 mouse model of amyotrophic lateral sclerosis (Kieran *et al*., 2004; Kalmar *et al*., 2008). Therefore, to investigate the effects of arimoclomol on mice with spinal and bulbar muscular atrophy, a daily intraperitoneal injected dose of 120 mg/kg/body weight was given after the onset of symptoms in AR100 mice, at 12 months of age, for a period of 16 days. Arimoclomol was shown to significantly upregulate the levels of Hsp70 both in spinal cord (a 2.3-fold increase) and the hindlimb tibialis anterior muscles (a 3-fold increase) of AR100 mice (Fig. 2A and B). The levels of Hsp90 were modestly increased but were not statistically significant. Interestingly, in tibialis anterior muscles, unlike the spinal cord, vehicle-treated symptomatic AR100 mice at 12 months of age displayed a higher level of Hsp70 compared with wild-type mice, which may be a reflection of a dissimilar response to stress present in the two tissues. In contrast, upregulation of Hsp70 or Hsp90 was not observed in either the cortex or the liver, tissues that are largely unaffected in spinal and bulbar muscular atrophy (Fig. 2C).

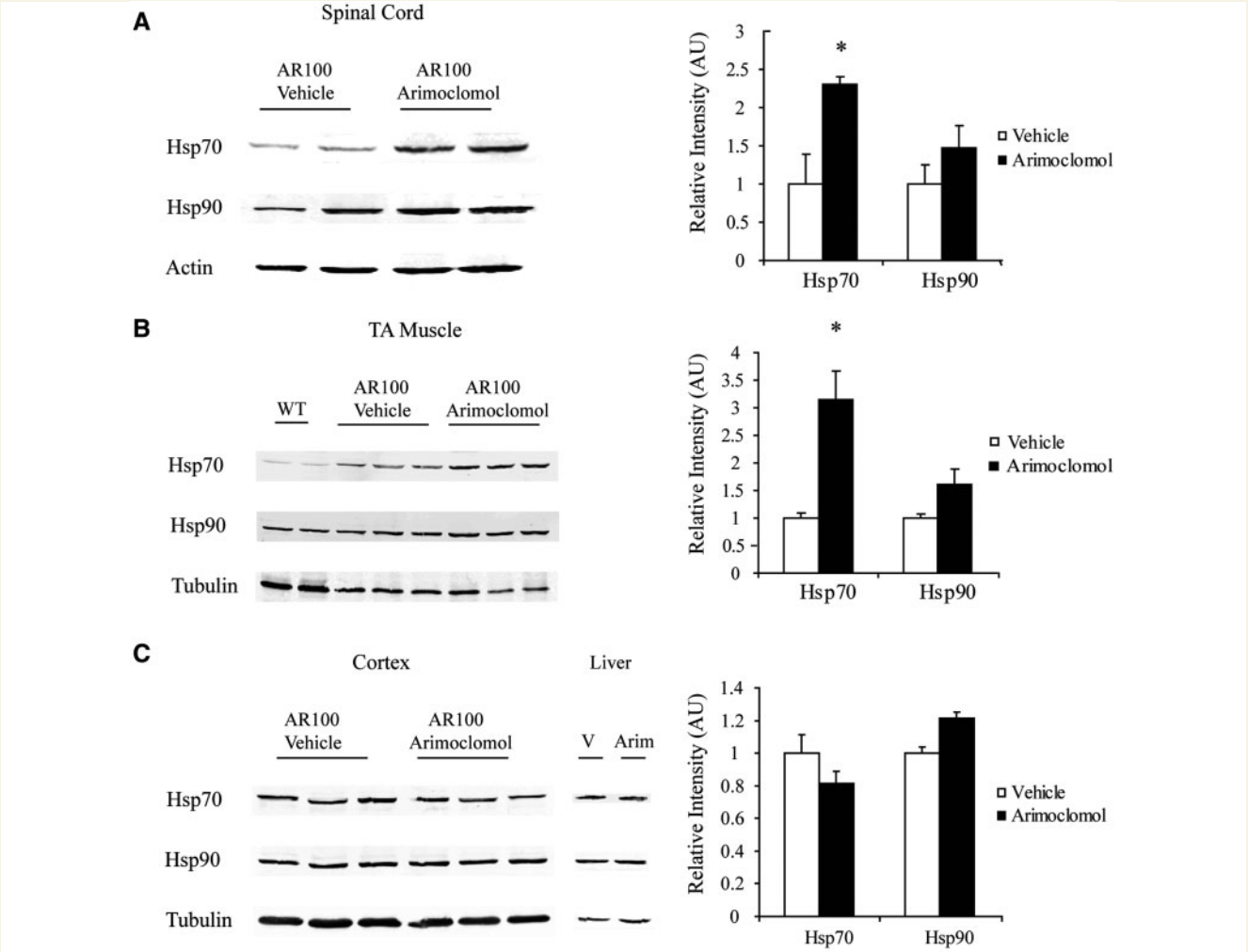

Figure 2 Arimoclomol induces heat shock proteins in spinal and bulbar muscular atrophy mice. To investigate the effects of arimoclomol, an intraperitoneal injected dose of 120 mg/kg/body weight was given daily to 12-month-old AR100 mice after the onset of symptoms for a period of 16 days. Arimoclomol significantly upregulated the expression of Hsp70 in (**A**) spinal cord and (**B**) hindlimb tibialis anterior (TA) muscles in comparison with vehicle-treated (WT) mice. Furthermore, no increase was observed in (**C**) cortex or liver of AR100 mice. Data are displayed as mean ± SEM and are representative of three independent experiments. Statistical analysis was performed using either a two sample *t*-test or one-way ANOVA followed by the Student–Newman–Keuls and Tukey's Honestly Significantly Different *post hoc* tests ($n \geqslant 3$, $^*P < 0.05$). Arim = arimoclomol; V = vehicle; AU = arbitrary units.

Arimoclomol treatment upregulates vascular endothelial growth factor in mice with spinal and bulbar muscular atrophy

The messenger RNA levels of vascular endothelial growth factor (Vegf), and in particular the Vegf164 splice variant, have previously been shown to be decreased in AR100 mice (Sopher *et al*., 2004). We hypothesized that arimoclomol in conjunction with its effect on the heat shock response may impart its beneficial effect by influencing other pathways. Therefore, the messenger RNA levels of several genes were examined using quantitative PCR. We assessed the levels of the transcription factor hypoxia inducible factor 1 (Hif1a), Vegf, sirtuin 1 (Sirt1), insulin-like growth factor (Igf1) and peroxisome proliferator-activated receptor-γ co-activator 1α, (Ppargc1a). Our results show that arimoclomol treatment significantly upregulated the levels of vascular endothelial growth factor, both in the spinal cord and hindlimb muscles of AR100 mice (Fig. 3A and B)

Physiological characterization of the neuromuscular phenotype of mice with spinal and bulbar muscular atrophy

The disease phenotype in the AR100 mouse model has been shown to closely follow the pattern of disease observed in patients with spinal and bulbar muscular atrophy, with a loss of motor neurons in the sciatic motor pool in the spinal cord in diseased mice accompanying the decline in neuromuscular function

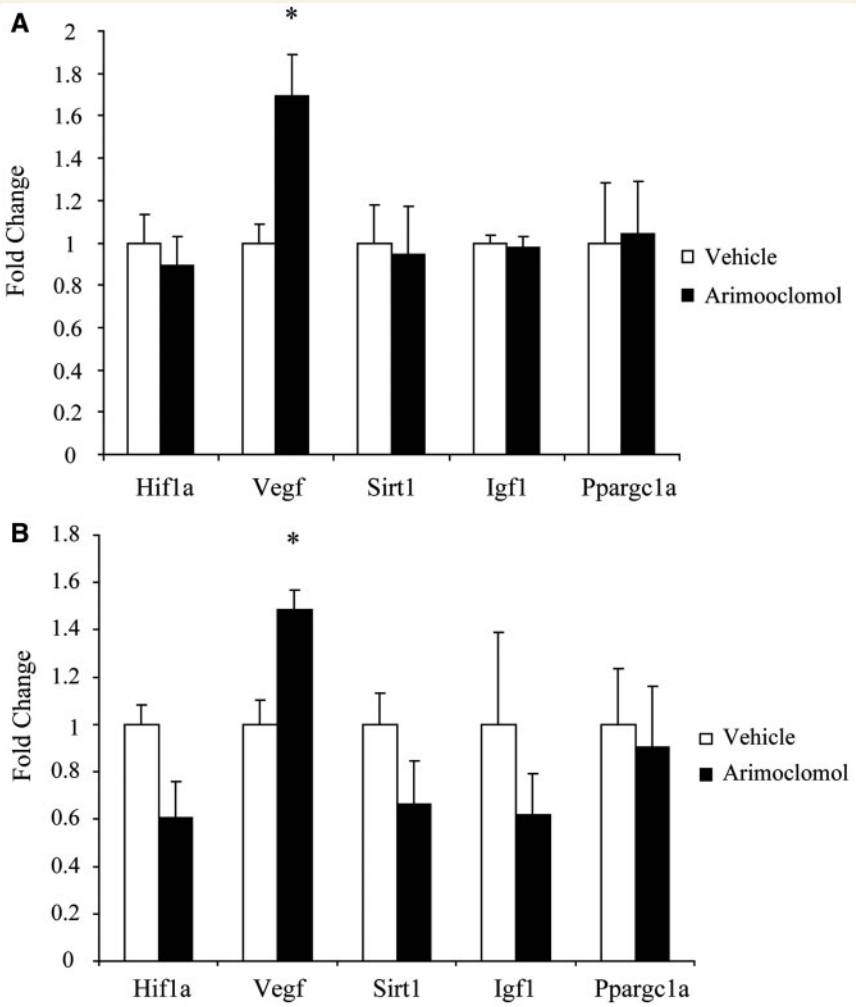

Figure 3 Arimoclomol upregulates vascular endothelial growth factor (Vegf) in spinal cord and muscles of mice with spinal and bulbar muscular atrophy. The expression of several genes was investigated using quantitative PCR after treatment with arimoclomol, with an intraperitoneal injected dose of 120 mg/kg/body weight given daily to 12-month-old AR100 mice after the onset of symptoms for a period of 16 days. There was a significant increase in levels of vascular endothelial growth factor both in (**A**) spinal cord and (**B**) hindlimb tibialis anterior muscles after administration of arimoclomol compared with vehicle-treated AR100 mice. Data are displayed as mean ± SEM and are representative of three independent experiments. Statistical analysis was performed using a two sample *t*-test ($n \geqslant 3$, $*P < 0.05$).

(Sopher *et al*., 2004; Malik *et al*., 2011). Although these mice have been previously evaluated using behavioural analysis (Sopher *et al*., 2004), in order to fully characterize the motor deficits, in this study we undertook an *in vivo* physiological examination of muscle function of specific hindlimb muscles in untreated heterozygote AR100 male mice at a late stage of disease (18 months), as well as male control AR20 mice that carry non-pathogenic 20 polyglutamine androgen receptor repeats and compared the findings with age-matched wild-type littermates. In addition, we also examined the phenotype of homozygote AR100 mice at 13 months of age, when these mice appeared to show a similar disease phenotype to that observed in 18-month heterozygote AR100 mice.

In vivo assessment of muscle force characteristics of the hindlimb muscles demonstrated that in heterozygote AR100 mice by 18 months of age, the twitch force in the tibialis anterior muscles was reduced by ~70% (12.40 ± 0.96 g, $n = 11$; $P < 0.05$) in comparison with wild-type mice (41.85 ± 4.24 g, $n = 8$). Tibialis anterior muscles remained unaffected in control AR20 mice (43.61 ± 2.01 g, $n = 11$; Fig. 4A). There was also a significant reduction in tibialis anterior muscle maximal tetanic force in AR100 mice, representing a decline of >50% (70.31 ± 3.30 g; $P < 0.05$) relative to wild-type mice (131.68 ± 4.97 g). No reduction in tibialis anterior muscle tetanic force was observed in AR20 mice (112.60 ± 7.19 g; Fig. 4B). Muscle force was also reduced in extensor digitorum longus muscles of 18-month-old AR100 mice, so that twitch force was 60% less (4.46 ± 0.45 g, $P < 0.05$) than extensor digitorum longus in either wild-type (10.88 ± 0.55 g) or AR20 mice (13.09 ± 1.40 g; Fig. 4E), and extensor digitorum longus tetanic force was 35% less in AR100 mice (20.31 ± 1.28 g, $P < 0.05$) than wild-type (30.67 ± 1.43 g) and AR20 mice (35.54 ± 2.29 g; Fig. 4F).

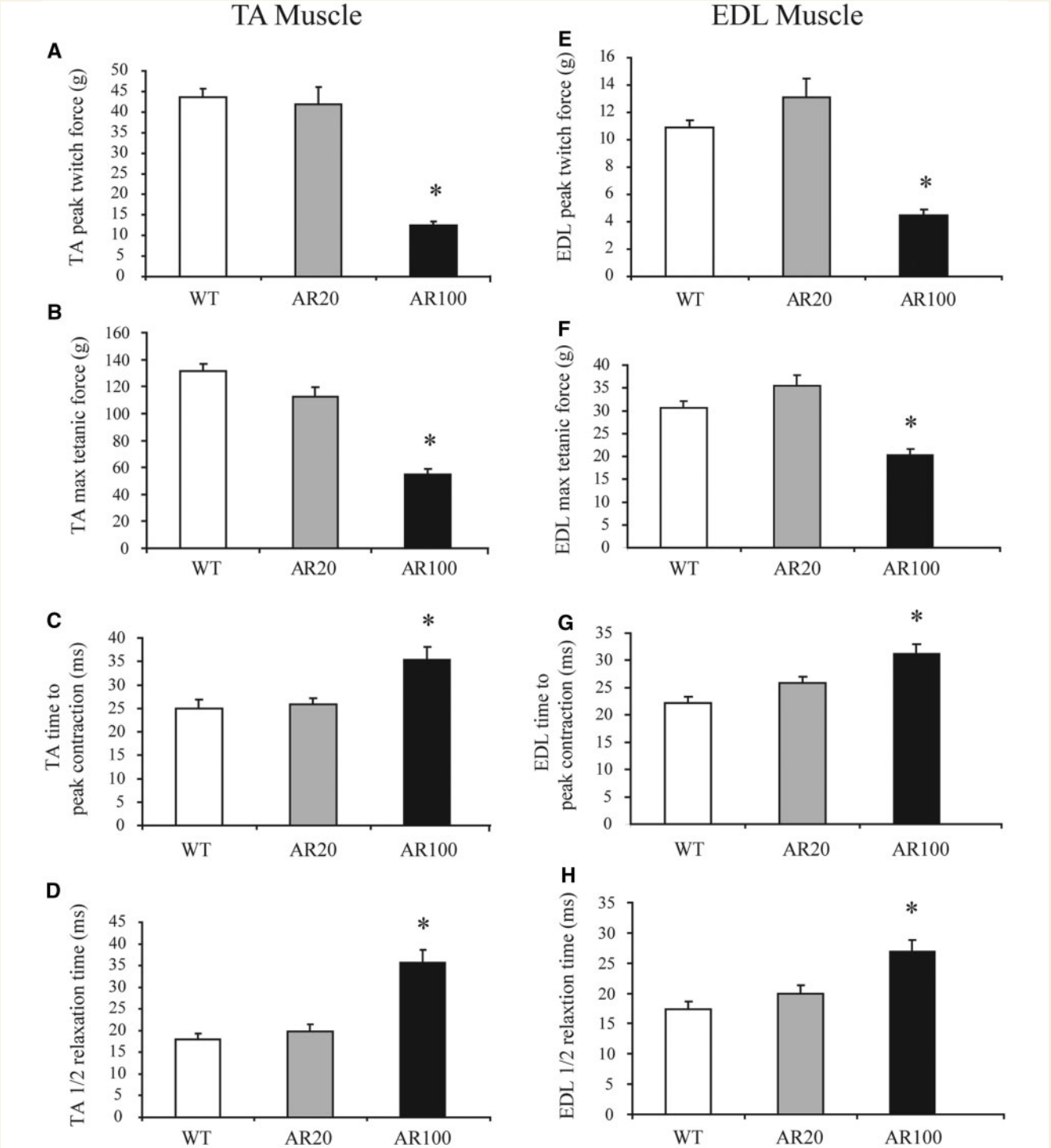

Figure 4 Deterioration of muscle force in hindlimb muscles of mice with spinal and bulbar muscular atrophy. *In vivo* assessment of hindlimb muscle force revealed a reduction in (**A**) maximal twitch and (**B**) tetanic tension in tibialis anterior (TA) muscles of 18-month-old AR100 mice ($n = 11$) compared with AR20 ($n = 11$) and wild-type (WT) mice ($n = 8$). Analysis of twitch contraction and relaxation rates of hindlimb muscles showed significant slowing of (**C**) tibialis anterior muscle time to peak contraction and (**D**) tibialis anterior muscle half relaxation time, indicative of muscle deterioration. In extensor digitorum longus (EDL) muscles, a similar loss of (**E**) twitch and (**F**) tetanic tension was also observed in AR100 mice, as well as a slowing of (**G**) the time to peak contraction and (**H**) half relaxation time. Values are expressed as mean ± SEM. Statistical analysis was performed using the Kruskal–Wallis test, $^*P < 0.05$.

The contractile characteristics of fast twitch muscles change in spinal and bulbar muscular atrophy mice

Fast twitch muscle fibres normally contract and relax rapidly. However, this characteristic has been shown to change in mouse models of motor neuron degeneration such as SOD1 mice, in which fast twitch muscles begin to show contractile characteristics that resemble those of slow twitch muscles (Kieran *et al*., 2004; Kalmar *et al*., 2008). We therefore examined the contractile characteristics of fast twitch muscles in 18-month-old AR100 mice. Recording of twitch contraction and relaxation rates of tibialis anterior and extensor digitorum longus muscles demonstrated a significant slowing in the time to peak contraction in AR100 mice, but not AR20 mice, in comparison with wild-type mice (Fig. 4C and G). Similarly, the half relaxation time was also markedly reduced in tibialis anterior and extensor digitorum longus muscles of AR100 mice, but not AR20 mice (Fig. 4D and H).

Fast twitch muscles such as extensor digitorum longus normally fatigue rapidly and cannot maintain force when repeatedly stimulated. We therefore examined the fatigue characteristics of extensor digitorum longus muscles in 18-month-old AR100 mice, by undertaking a fatigue test in which the muscles were repeatedly stimulated. Typical fatigue traces from extensor digitorum longus muscles of wild-type, AR100 and AR20 mice are shown in Fig. 5A, which shows that in AR100 mice, there was a clear shift in the fatigue pattern of extensor digitorum longus, which became fatigue resistant. From traces such as these, a fatigue index was calculated for each muscle, where a fatigue index of 1.0 indicates that a muscle is completely fatigable. Our findings show that in AR100 mice the extensor digitorum longus fatigue index was reduced by 63% (0.30 ± 0.05, $P < 0.05$) in comparison with extensor digitorum longus in wild-type (0.82 ± 0.02) and AR20 mice (0.73 ± 0.06; Fig. 5A). These results show that in AR100 animals, extensor digitorum longus muscles are significantly more fatigue-resistant than those of wild-type or AR20 animals, a characteristic more usually observed in slow twitch muscles.

Loss of functional motor units in mice with spinal and bulbar muscular atrophy and progressive nature of disease

The number of functional motor units innervating the extensor digitorum longus muscles was determined by stimulating the sciatic nerve with stimuli of increasing intensity, resulting in stepwise increments in twitch tension due to successive recruitment of motor axons. Typical examples of motor unit traces from extensor digitorum longus muscles of wild-type and AR100 mice are shown in Fig. 2B. In 18-month-old AR100 mice, there was a 31% reduction in the number of motor units in extensor digitorum longus muscles of AR100 mice (25.6 ± 0.8, $P < 0.05$) than in age matched wild-type (37.2 ± 1.2) and AR20 mice (35.8 ± 2.5; Fig. 5B), indicative of significant motor neuron degeneration.

In addition, we evaluated physiological muscle function in presymptomatic mice and found no impairment in hindlimb muscle function in 3-month-old mice with spinal and bulbar muscular atrophy compared with age matched wild-type littermates (Fig. 5C–F). In contrast, 18-month-old mice with spinal and bulbar muscular atrophy show significant neuromuscular deficits and therefore demonstrate the presence of a progressive neuromuscular phenotype in AR100 mice.

Loss of muscle weight and changes in muscle fibre phenotype of fast twitch muscles in mice with spinal and bulbar muscular atrophy

At the end of the acute physiological experiments, the hindlimb muscles were removed, weighed and processed for histochemical analysis. In 18-month-old AR100 mice, tibialis anterior muscles weighed significantly less (31.39 ± 1.3 mg, $P < 0.05$) than in wild-type (58.27 ± 1.48 mg) and AR20 mice (53.73 ± 2.9 mg; Fig. 6A). Similarly, extensor digitorum longus muscle weight was markedly reduced in AR100 mice (7.18 ± 0.34 mg, $P < 0.05$) relative to wild-type (12.03 ± 0.38 mg) and AR20 mice (11.59 ± 0.69 mg; Fig. 6A). Interestingly, no change was observed in the weight of the slow twitch soleus muscle (Fig. 6A), a muscle that is known to be more resistant to disease in the mutant SOD1 mouse model of amyotrophic lateral sclerosis (Kieran *et al*., 2004; Sharp *et al*., 2005). Furthermore, physiological assessment of muscle force characteristics was also assessed at an earlier presymptomatic stage of the AR100 mice. No perturbation of hindlimb muscle physiology was found in these mice, which therefore highlights the slowly progressive nature of the disease in spinal and bulbar muscular atrophy AR100 mice (Fig. 6C–F).

Therefore, fast twitch muscles in AR100 mice develop fatigue characteristics normally observed in slow twitch muscles. A similar switch in the phenotype of fast twitch muscles has previously been reported in mutant SOD1 amyotrophic lateral sclerosis mice (Kieran *et al*., 2004).

Motor neuron survival

Following removal of the hindlimb muscles, the mice were terminally anaesthetized, perfused with fixative and the lumbar spinal cord was removed and processed for analysis of motor neuron survival. An example of a ventral horn of a spinal cord section from an 18-month-old AR100 mouse in which degenerating motor neurons are visible, is shown in Fig. 3B. As we have previously reported (Malik *et al*., 2011), in AR100 mice by 18 months of age, 40% of motor neurons have died in the sciatic motor pool of the spinal cord compared with age-matched wild-type mice or AR20 mice, in which no motor neuron death was detected (Fig. 6C). Thus, in heterozygote AR100 mice, the decline in muscle function is associated with a significant degeneration of spinal motor neurons, a phenotype that mirrors that observed in patients with spinal and bulbar muscular atrophy.

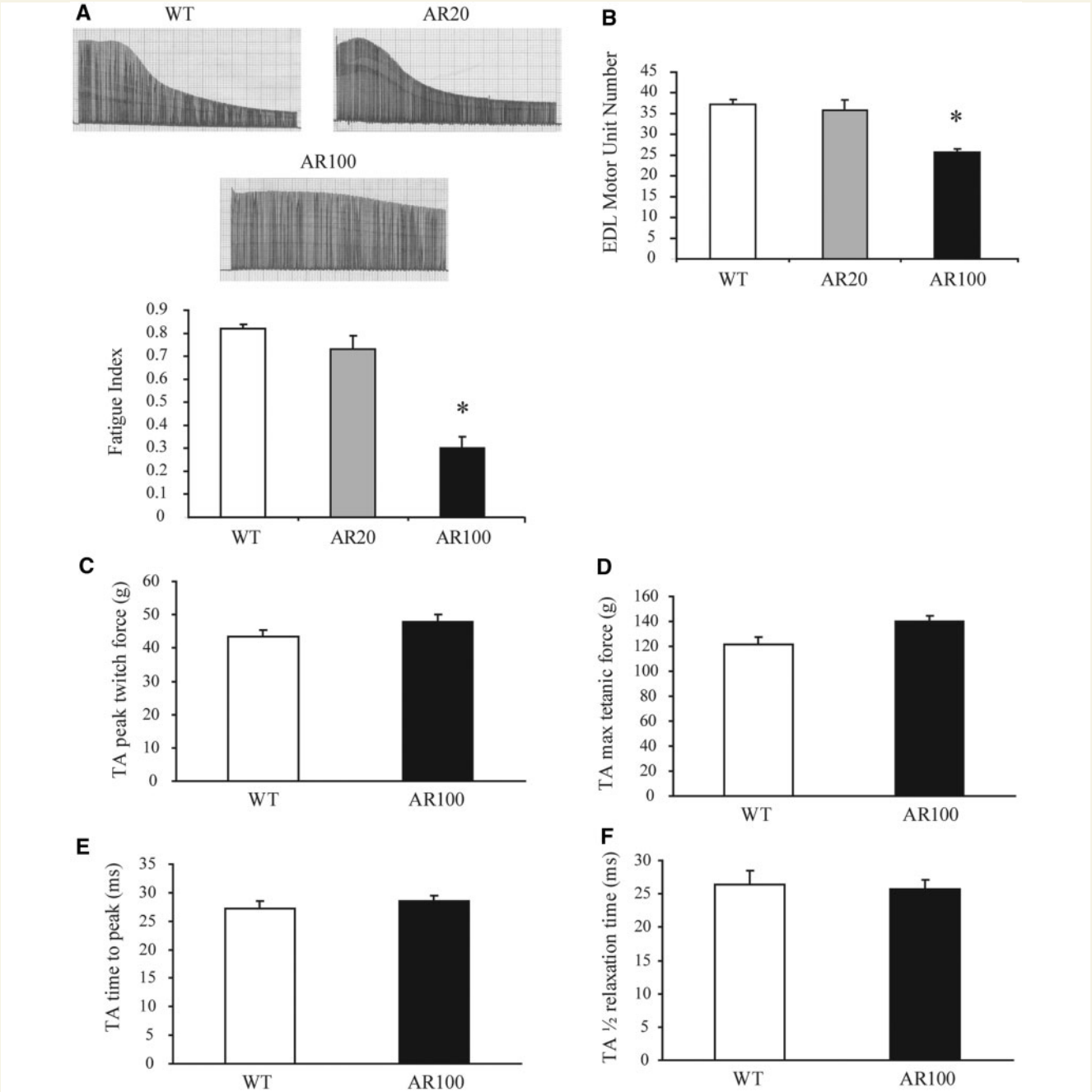

Figure 5 Development of a progressive neuromuscular phenotype in mice with spinal and bulbar muscular atrophy, manifested by a loss of motor units and the development of abnormal muscle fatigue characteristics. (**A**) The fatigue characteristics of extensor digitorum longus (EDL) muscles in 18-month-old AR100 mice ($n = 11$) compared with AR20 ($n = 11$) and wild-type (WT) mice ($n = 8$) were examined. As can be seen in the fatigue traces, in AR100 mice, the extensor digitorum longus muscles become resistant to fatigue and can maintain force when repeatedly stimulated. From such traces, a fatigue index was calculated for each muscle, where a fatigue index of 1.0 indicates that a muscle is completely fatigue resistant. The bar chart shows that there a significant decrease in the fatigue index of AR100 extensor digitorum longus muscles. (**B**) The number of functional motor units innervating extensor digitorum longus was established. Typical motor unit traces from extensor digitorum longus muscles of 18-month-old wild-type, AR20 and AR100 mice are shown. Motor unit numbers were significantly reduced in extensor digitorum longus muscle of AR100, but not AR20 mice. Analysis of muscles was also performed in presymptomatic 3-month-old mice, which showed no pathological alteration in (**C**) maximal twitch and (**D**) tetanic tension, or (**E**) the time to peak contraction and (**F**) half relaxation time in tibialis anterior muscle (TA). Values are expressed as mean ± SEM. Statistical analysis was performed using the Kruskal–Wallis test, $*P < 0.05$.

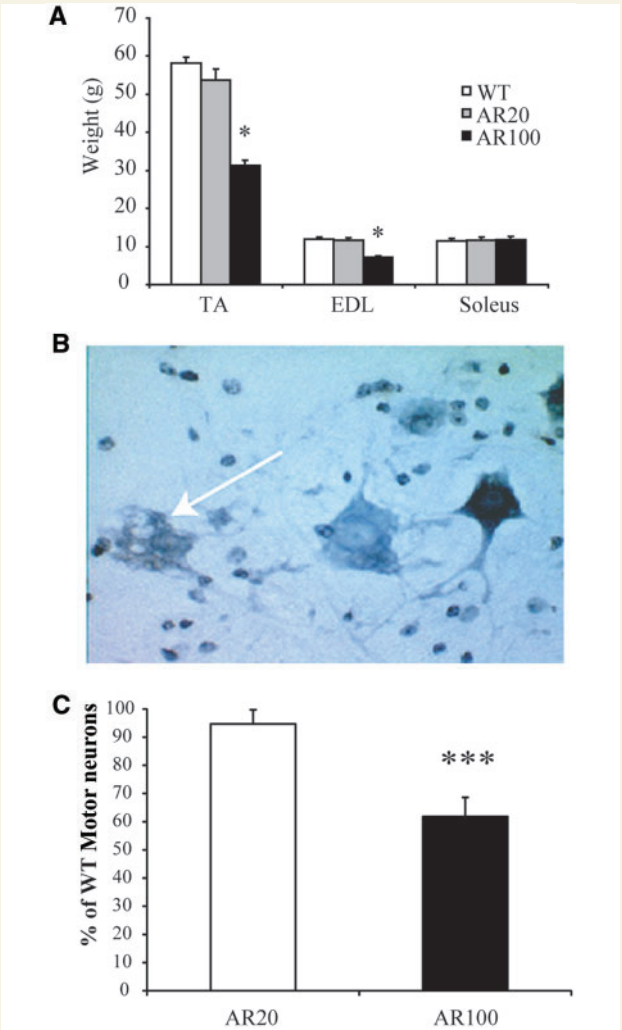

Figure 6 Pathological changes in muscle and spinal cord of mice with spinal and bulbar muscular atrophy. (**A**) The mean weight of tibialis anterior muscles (TA), extensor digitorum longus (EDL) and soleus muscles of wild-type, AR20 and AR100 mice shows a significant decrease in the weight of fast twitch muscles in 18-month-old AR100 mice, but not in slow twitch muscles such as soleus. (**B**) The presence of degenerating motor neurons can be observed in the ventral horn of 18-month-old AR100 mice (arrow indicates degenerating neuron). (**C**) Surviving motor neurons in the ventral horn sciatic motor pool were counted and the results shown in the bar chart, with values expressed as a percentage of wild-type surviving motor neurons. By 18 months of age, a significant number of motor neurons have died in AR100 mice compared with wild-type (WT), whereas no motor neuron death occurs in AR20 mice. For each genotype, $n \geqslant 7$, with one-way ANOVA and *post hoc* analysis performed to test for significance, with $*P < 0.05$ and $***P < 0.001$; error bars represent SEM.

Disease progression in AR100 homozygote mice

We also examined yeast artificial chromosome AR100 mice homozygous for the expanded polyglutamine androgen receptor. These mice exhibited signs of hindlimb dysfunction at a significantly earlier age than heterozygote AR100 mice. Physiological analysis of muscle function showed that 13-month-old homozygote AR100 mice demonstrated a pathology comparable with that observed in 18-month-old AR100 mice, with a dramatic reduction in twitch and tetanic muscle force, as well as impaired hindlimb muscle contractile properties (Supplementary Fig. 1). AR100 homozygotes also showed a significant reduction in motor unit number, aberrant muscle fatigue profiles and muscle atrophy, similar to that observed in 18-month heterozygote AR100 mice (Supplementary Fig. 2). Therefore, an extra copy of the mutant expanded *AR* gene in homozygous mice resulted in an accelerated disease phenotype, which likely stems from increased expression of the mutant protein. These results highlight the pathogenic and toxic gain of function properties of the expanded androgen receptor.

Collectively, these results show that AR100 mice develop severe atrophy of fast hindlimb muscles and additionally demonstrate a deficit in fatigue resistance associated with loss of innervating motor units. Therefore, the AR100 mice develop a polyglutamine-dependent neuromuscular phenotype characterized by a decline in the number of functional motor units and muscle atrophy.

Upregulation of the heat shock response improves neuromuscular function and rescues motor neurons in mice with spinal and bulbar muscular atrophy

We have previously shown that targeting of the heat shock response by treatment with arimoclomol, a novel heat shock protein co-inducer, delays disease progression and improves the neuromuscular deficit in a mutant SOD1 mouse model of amyotrophic lateral sclerosis (Kieran *et al*., 2004; Kalmar *et al*., 2008), a disease in which motor neuron degeneration is the defining characteristic. Since arimoclomol acts by augmenting the heat shock response and upregulating the expression of several cytoprotective heat shock proteins, it is possible that upregulation of this ubiquitous cellular defence pathway may also be beneficial in spinal and bulbar muscular atrophy. Therefore, treatment of heterozygote AR100 mice with arimoclomol at a daily oral dose of 120 mg/kg/body weight was commenced after the onset of symptoms in AR100 mice, at 12 months of age, and continued until the designated end point of the study, at 18 months, the stage where untreated AR100 mice are severely affected and manifest a serious impairment of neuromuscular function.

As a general measure of disease progression, body weight was recorded throughout the study. After initially gaining weight, untreated AR100 diseased animals showed a gradual, but significant, decline in body weight concurrent with disease progression (Fig. 7A). However, treatment with arimoclomol significantly reduced the decline in body weight of AR100 mice, and even at 18 months, they were still 15% heavier ($P < 0.05$) than untreated AR100 mice (Fig. 7A). Furthermore, the muscle wasting and overt kyphosis of the vertebral column observed in AR100 mice at 18 months (Sopher *et al*., 2004) was less apparent in arimoclomol-treated mice.

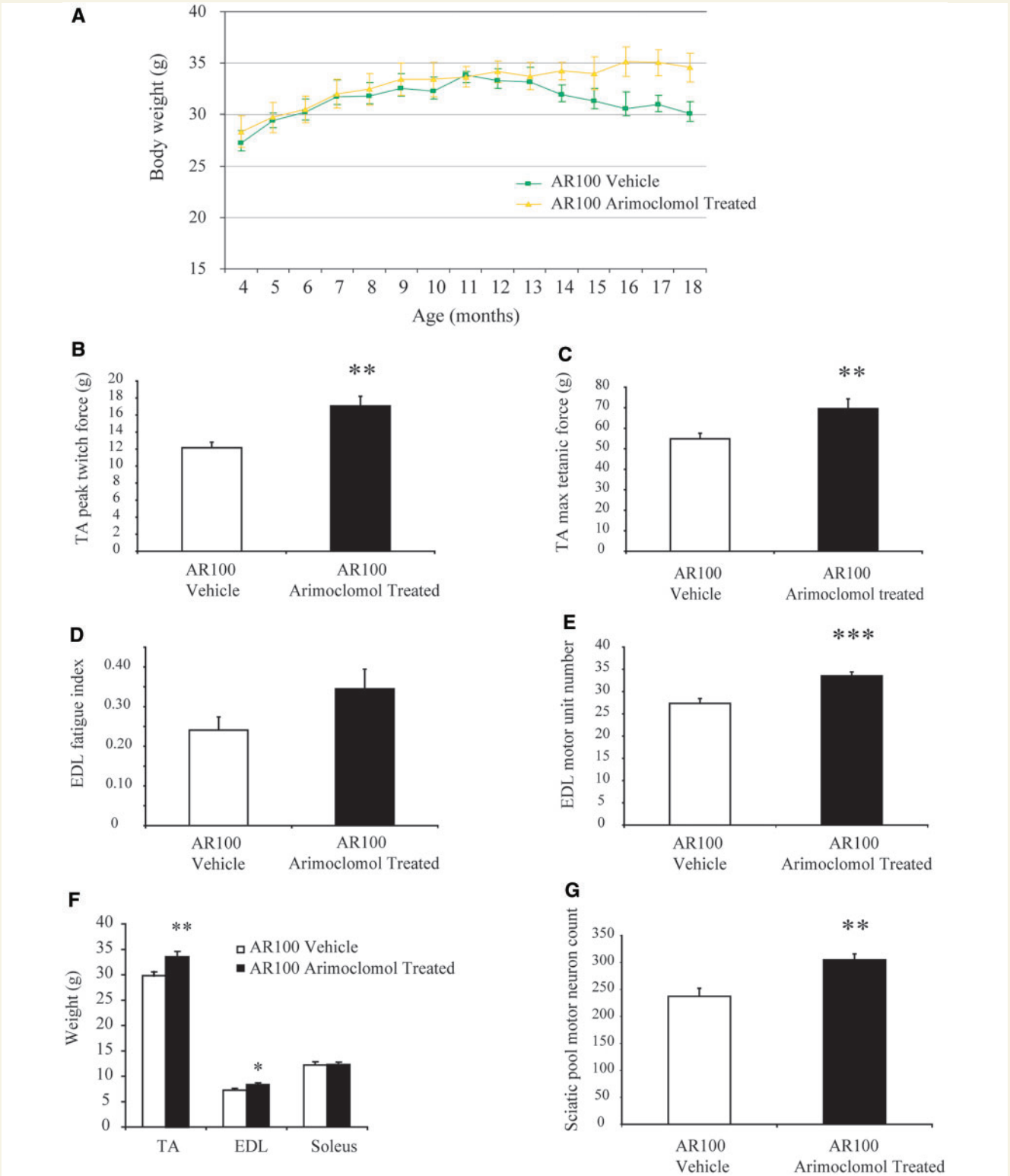

Figure 7 Treatment with arimoclomol delays disease progression in mice with spinal and bulbar muscular atrophy. (**A**) Body weight was recorded monthly from 4–18 months of age in arimoclomol and vehicle-treated AR100 mice. Body weight begins to decline from 13 months in vehicle-treated AR100 mice, but is maintained in mice treated with arimoclomol. Arimoclomol increased the maximal (**B**) twitch tension and (**C**) maximal tetanic force in tibialis anterior (TA) muscles of AR100 mice ($n = 10$) compared with vehicle-treated mice ($n = 8$) at 18 months of age. (**D**) Arimoclomol prevents the change in the fatigue characteristics and (**E**) increases motor unit survival in extensor digitorum longus muscles of AR100 mice. (**F**) There is a significant increase in the weight of tibialis anterior and extensor digitorum longus muscles (EDL) in arimoclomol-treated AR100 mice, but no change in the soleus muscle, which is unaffected in AR100 mice at this stage. (**G**) These improvements in muscle function in arimoclomol-treated AR100 mice are reflected in a significant increase in motor neuron survival. Values are expressed as mean ± SEM. Statistical analysis was performed using the Mann–Whitney U test, $*P < 0.05$, $**P < 0.01$ and $***P < 0.001$.

To establish the effects of arimoclomol on the neuromuscular phenotype of AR100 mice, at 18 months of age, arimoclomol-treated AR100 mice ($n = 10$) and vehicle-treated controls ($n = 8$) were prepared for *in vivo* examination of muscle force. In AR100 mice treated with arimoclomol, there was a 40% improvement in the twitch force of tibialis anterior muscles compared with untreated AR100 mice (17.07 ± 1.12 g and 12.15 ± 0.65 g, respectively, $P < 0.01$; Fig. 7B). There was also a significant improvement in the maximal tetanic force of tibialis anterior muscles in arimoclomol-treated AR100 mice, which were 26.9% stronger than tibialis anterior muscles in untreated AR100 mice (69.57 ± 4.76 g and 54.83 ± 2.69 g, respectively, $P < 0.01$; Fig 7C).

Furthermore, we show that treatment with arimoclomol has no effect on muscle force of wild-type mice, which do not show any pathology (Supplementary Fig. 3). This observation suggests that beneficial effects of arimoclomol are likely to be due to amelioration of the pathogenic process occurring in the spinal cord and not as a result of indiscriminate improvement of muscle force.

There was a similar improvement in twitch and tetanic force of extensor digitorum longus muscles in arimoclomol-treated AR100 mice. Thus twitch force was 39% greater in arimoclomol-treated compared with untreated AR100 mice (4.99 ± 0.45 g and 3.59 ± 0.25 g, respectively, $P < 0.05$; Supplementary Fig. 4A), and tetanic force was 18.9% greater in arimoclomol-treated mice than in control subjects (20.80 ± 1.72 g and 17.50 ± 1.74 g, respectively; Supplementary Fig. 4B), although this improvement was not statistically significant ($P = 0.18$).

Despite the improvements in muscle force observed in arimoclomol-treated AR100 mice, there was no improvement in the contractile characteristics in either the extensor digitorum longus or tibialis anterior muscles, which were significantly reduced in AR100 mice (Supplementary Fig. 4C–F). Furthermore, the fatigue pattern of extensor digitorum longus muscles in arimoclomol-treated AR100 mice indicated that these muscles were slightly fatigable (Supplementary Fig. 4G). However, calculation of the fatigue index showed that although the fatigue index in arimoclomol-treated extensor digitorum longus muscles resembled that of wild-type mice and represented a clear improvement of 43% from vehicle-treated AR100 mice, it was not statistically significant ($P = 0.083$; Fig. 7D).

To assess the effect of arimoclomol on the survival of functional motor units, the number of motor units innervating the extensor digitorum longus muscles of arimoclomol-treated and vehicle control animals was determined. As shown in Fig. 4E, there was a 23% improvement in motor unit survival in arimoclomol-treated AR100 mice, in which 33.5 ± 0.9 motor units survived compared with 27.3 ± 1.1 in untreated AR100 mice ($P < 0.001$; Fig. 7E).

At the end of the physiological assessment of neuromuscular function, the hindlimb muscles were removed and weighed. In arimoclomol-treated AR100 mice, there was a significant increase in the weight of both extensor digitorum longus and tibialis anterior muscles. Thus, in treated mice, tibialis anterior muscles weighed 33.48 ± 1.10 mg compared with 28.93 ± 0.68 mg in untreated AR100 mice ($P < 0.01$) and extensor digitorum longus weighed 8.36 ± 0.36 mg in treated mice compared with 7.27 ± 0.30 mg in untreated AR100 mice ($P < 0.05$; Fig. 7F). As observed in untreated AR100 mice, soleus muscles in arimoclomol-treated mice weighed the same as soleus muscles of wild-type mice (Fig. 6A).

Since we have previously shown that there is a significant loss of motor neurons in 18-month-old AR100 mice (Malik *et al*., 2011), we also examined the effects of arimoclomol on motor neuron survival. The number of motor neurons surviving in the sciatic motor pool was established, and the results showed that in arimoclomol-treated AR100 mice, 28.4% more motor neurons survived (304.8 ± 29.1) than in untreated AR100 mice (237.3 ± 39.3; $P < 0.01$; Fig. 7G).

Taken together, these results show that in mice with spinal and bulbar muscular atrophy, long-term treatment with arimoclomol, between 12–18 months of age, is not only safe and well-tolerated but also results in a significant improvement in neuromuscular function and motor neuron survival, the hallmark pathology in patients with spinal and bulbar muscular atrophy.

Discussion

Our results show that AR100 transgenic mice develop a progressive hindlimb paralysis, caused by motor neuron degeneration, and thus recapitulate human spinal and bulbar muscular atrophy. AR100 mice therefore represent an excellent animal model in which to test novel therapeutic strategies for spinal and bulbar muscular atrophy. We found that treatment of AR100 mice with an oral dose of arimoclomol significantly delayed disease progression by preventing motor neuron degeneration, thereby improving the survival of functional motor units, reducing atrophy of hindlimb muscles and attenuating the deterioration in body weight. Importantly, these beneficial effects of arimoclomol were observed even though treatment with arimoclomol commenced after symptom onset. In addition, arimoclomol upregulated the expression level of the neurotrophic factor, Vegf, both in the spinal cord and hindlimb muscles. Therefore, our study provides compelling evidence that treatment with arimoclomol, a novel co-inducer of the heat shock response that we have previously shown to be effective in delaying disease progression in a mouse model of amyotrophic lateral sclerosis (Kieran *et al*., 2004; Kalmar *et al*., 2008), may also be a potential therapeutic strategy in the treatment of spinal and bulbar muscular atrophy.

We first evaluated the expression of heat shock proteins in the AR100 mouse model of spinal and bulbar muscular atrophy because the levels of these proteins have been reported to be decreased in polyglutamine repeat expansion diseases (Adachi, 2003; Katsuno, 2005; Labbadia *et al*., 2011). Our results show that there is a decrease in Hsp70 expression in the spinal cord of mice with late stage disease spinal and bulbar muscular atrophy. Furthermore, treatment with arimoclomol results in a significant increase in the expression of Hsp70 in both the spinal cord and hindlimb muscles, but importantly arimoclomol treatment does not alter heat shock protein expression in tissues unaffected by pathology in spinal and bulbar muscular atrophy, such as the cortex or liver.

To fully assess the effects of arimoclomol in the AR100 mouse model of spinal and bulbar muscular atrophy, we undertook a comprehensive physiological characterization of hindlimb

neuromuscular function in AR100 mice. Although AR100 mice have previously been shown to exhibit a slowly progressive phenotype without a dramatic reduction in lifespan (Sopher *et al*., 2004), this study did not include a detailed physiological analysis of hindlimb muscle function. Our findings show that in AR100 mice, neuromuscular function is severely compromised, in a polyglutamine-dependent manner. We found a significant decrease in muscle force in fast twitch hindlimb muscles coupled with an abnormal pattern of muscle contractile and fatigue characteristics, loss of functional motor units innervating the hindlimb muscles and muscle atrophy. These deleterious changes manifest significantly earlier in AR100 mice homozygous for the expanded polyglutamine androgen receptor than in heterozygote AR100 mice. Degeneration of motor neurons in the lumbar spinal cord is a fundamental feature of spinal and bulbar muscular atrophy (Katsuno *et al*., 2004; Adachi *et al*., 2005) and importantly, this defining characteristic of spinal and bulbar muscular atrophy is recapitulated in AR100 mice, which show a significant loss of motor neurons in the sciatic motor pool (Katsuno *et al*., 2002; Chevalier-Larsen *et al*., 2004; Sopher *et al*., 2004; Yu *et al*., 2006; Malik *et al*., 2011).

Using the AR100 mouse model of spinal and bulbar muscular atrophy, we have shown that treatment of AR100 mice with an oral dose of arimoclomol significantly delayed disease progression. This is accordingly reflected in a reduction in motor neuron degeneration, an improvement in motor unit survival, a reduction in hindlimb muscle atrophy and an attenuation in the deterioration in body weight. These may be as a result of arimoclomol's beneficial effects both in the periphery in muscles under stress, as well as in motor neurons within the CNS. Additionally, treatment with arimoclomol had no impact on muscle physiology of unaffected wild-type mice. Taken together these observations suggests that beneficial effects of arimoclomol are likely to be due in part to the amelioration of the pathogenic process occurring in spinal cord and not as a result of indiscriminate improvement of muscle force. Arimoclomol is an attractive therapeutic candidate for spinal and bulbar muscular atrophy, as it has already been shown to be safe and well tolerated in healthy volunteers and patients with amyotrophic lateral sclerosis (Cudkowicz *et al*., 2008), a more aggressive and usually fatal motor neuron disease, and is currently undergoing a phase II/III trial in the USA in SOD1-positive patients with amyotrophic lateral sclerosis (www.ClinicalTrials.gov). Furthermore, the outcome of two recent randomized placebo-controlled studies evaluating therapies for spinal and bulbar muscular atrophy yielded mixed results (Katsuno *et al*., 2010*b*), highlighting the urgent need for an effective disease-modifying therapy for spinal and bulbar muscular atrophy with limited side effects.

There is now a significant body of evidence that indicates that manipulation of the heat shock response, a well characterized cellular defence mechanism, should be an effective strategy for the treatment of both polyglutamine repeat expansion diseases and other more aggressive motor neuron disorders such as amyotrophic lateral sclerosis (Lanka *et al*., 2009; Ranganathan and Fischbeck, 2010). Components of the heat shock response including chaperones, as well as members of the ubiquitin–proteasome system degradative machinery, are present in polyglutamine nuclear inclusions and in inclusions in both SOD1-positive patients with amyotrophic lateral sclerosis and mutant SOD1 mice, suggesting a possible failure of these mechanisms in these disorders (Stenoien *et al*., 1999; Watanabe *et al*., 2001; Adachi *et al*., 2003; Crippa *et al*., 2010; Prudencio *et al*., 2010). Although aggregate formation is a common feature of several neurodegenerative diseases (Wood *et al*., 2003; Ross and Poirier, 2004), evidence suggests that the toxic species may in fact be oligomeric soluble forms of the mutant protein rather than aggregates of insoluble protein themselves. Thus, in spinal and bulbar muscular atrophy, the major polyglutamine pathogenic toxic species is thought to be an oligomeric soluble form of the androgen receptor. Therefore, diffuse nuclear accumulation of polyglutamine mutant proteins may be an early event that occurs prior to inclusion formation, with the presence of oligomeric micro-aggregates being toxic to motor neurons (Li *et al*., 2007; Takahashi *et al*., 2008). Interestingly, in the AR100 mice used in this study, no microscopically visible nuclear inclusion bodies can be detected in motor neurons, but rather a pattern of diffuse staining within the nucleus is observed (Sopher *et al*., 2004). This is similar to the diffuse nuclear accumulation found in human patients, the presence of which is one of the defining histopathological hallmarks of spinal and bulbar muscular atrophy (Adachi *et al*., 2005). Notably, oligomeric species have also been found in other mouse models of spinal and bulbar muscular atrophy as well as other polyglutamine repeat expansion disease models (Li *et al*., 2007; Takahashi *et al*., 2008).

Heat shock proteins are thought to reduce polyglutamine-mediated cytotoxicity by refolding and solubilizing the pathogenic proteins (Wyttenbach, 2004). Heat shock proteins prevent the initial conformational change of the abnormal polyglutamine-containing protein from a random coil to a β-sheet, leading to a decrease in toxic oligomer formation (Wyttenbach, 2004; Muchowski and Wacker, 2005). Therefore in spinal and bulbar muscular atrophy, activation of the heat shock response, either through genetic overexpression of heat shock proteins or by pharmacological induction, may prevent misfolding of pathogenic proteins and offer protection against the polyglutamine repeat expansion-linked toxicity (Kobayashi *et al*., 2000; Adachi *et al*., 2003; Katsuno *et al*., 2005; Fujikake *et al*., 2008). Polyglutamine repeat expansion proteins can also have a detrimental effect on the heat shock response, with truncated polyglutamine androgen receptor causing the failure of Hsp70 induction following heat shock (Cowan *et al*., 2003). Levels of heat shock proteins have also been reported to be reduced in mouse models of polyglutamine repeat expansion diseases, including spinal and bulbar muscular atrophy (Adachi, 2003; Katsuno, 2005; Labbadia *et al*., 2011). Thus, beneficial effects of heat shock proteins have been reported in cellular models of spinal and bulbar muscular atrophy, with overexpression of Hsp70 and Hsp40 resulting in a reduction in toxicity (Kobayashi *et al.,* 2000), and increased Hsp70 was found to facilitate proteosomal degradation of mutant androgen receptor protein (Bailey *et al*., 2002). Furthermore, in an AR-97Q mouse model of spinal and bulbar muscular atrophy, overexpression of human Hsp70 markedly improves the phenotype of the pathogenic mice (Adachi *et al*., 2003). Over-expression of the C terminus of Hsc70 (heat

shock cognate protein 70-interacting protein, CHIP), which interacts with Hsp90 and Hsp70, also alleviates the neuromuscular phenotype of AR-97Q spinal and bulbar muscular atrophy mice by reducing nuclear localization of pathogenic androgen receptor through enhanced degradation of the protein (Adachi *et al*., 2007).

However, these studies largely involved upregulation of individual or specific combinations of heat shock proteins, and it is possible that activation of multiple heat shock proteins and co-chaperones in a coordinated fashion may prove to be more effective in alleviating pathology in complex progressive disorders such as spinal and bulbar muscular atrophy. One compound that has been shown to have such broad effects on heat shock protein expression is geranylgeranylacetone, which has been reported to upregulate the levels of Hsp70, Hsp90 and Hsp105 via activation of HSF1 (Katsuno *et al*., 2005). In an AR-97Q mouse model of spinal and bulbar muscular atrophy, treatment with geranylgeranylacetone has been shown to inhibit mutant androgen receptor nuclear accumulation, resulting in amelioration of the neuromuscular phenotype of these mice (Katsuno *et al*., 2005). Targeted inhibition of Hsp90 has also proved effective in reducing the pathogenic phenotype in spinal and bulbar muscular atrophy mice (Waza *et al*., 2005). Hsp90, along with Hsp70, functions in a multi-chaperone complex and facilitates folding and assembly of its client proteins including the androgen receptor (Pratt, 1998). Treatment with 17-allylamino-17-demethoxygeldanamycin (17-AAG), an Hsp90 inhibitor, resulted in dissociation of the Hsp90–androgen receptor complex and directed degradation of the pathogenic androgen receptor by the proteasomal pathway in spinal and bulbar muscular atrophy (Waza *et al*., 2005). In addition, 17-dimethylaminoethylamino-17-demethoxygeldanamycin (17-DMAG), a more potent version of 17-AAG, has also been shown to have beneficial effects in a mouse model of spinal and bulbar muscular atrophy (Tokui *et al*., 2009). Mechanistically, Hsp90 inhibitors may also function to activate HSF1, by dissociation of HSF1 from the Hsp90 complex. However, there is documented evidence of adverse reactions after the administration of 17-AAG (Banerji *et al*., 2005), with an increased incidence of tumours (Price *et al*., 2005), likely due to disruption of interaction of Hsp90 client proteins other than androgen receptor.

Arimoclomol is a hydroxylamine derivative shown to result in the upregulation of a broad range of heat shock proteins via activation of HSF1 (Hargitai *et al*., 2003). However, in contrast to drugs previously tested in models of spinal and bulbar muscular atrophy, arimoclomol acts like a 'smart-drug' and only enhances the heat shock response in cells already under stress and in which the heat shock response is already activated (Vigh *et al*., 1997; Kalmar *et al*., 2008). Arimoclomol therefore selectively targets only cells exhibiting a stress response, significantly reducing the likelihood of non-specific side effects in otherwise unstressed cells, which have been observed following the use of direct activators of the heat shock response (Kalmar *et al*., 2008). Our data therefore show that arimoclomol treatment increased expression of Hsp70 only in affected tissue (spinal cord and muscle) and not in unaffected regions (cortex and liver). As a consequence of its ability to upregulate the heat shock response and thereby increase expression of several heat shock proteins and co-chaperones, arimoclomol can potentially target several pathological features of spinal and bulbar muscular atrophy, including the formation of the toxic oligomeric species of androgen receptor and its accumulation into micro-aggregates, as well as the formation of aggregates of misfolded proteins (Gabai *et al*., 1997; Wyttenbach, 2004; Ruchalski *et al*., 2006). Heat shock proteins can also target several other pathways that have been implicated in the degeneration of motor neurons in spinal and bulbar muscular atrophy, including the apoptotic pathway, by inhibition of cytochrome c release (Marfe *et al*., 2009) and the p38 MAP kinase pathway (Yamagishi *et al*., 2010), suppression of NF-κB-induced cell death (Bao and Liu, 2009) and reduction of oxidative stress (Qu *et al*., 2011).

Since arimoclomol acts by prolonging the activation of HSF1 (Hargitai *et al*., 2003), a transcription factor with several downstream targets (Page *et al*., 2006), it is possible that upregulation of heat shock proteins may not be the only mechanism underlying the beneficial effects of arimoclomol observed in models of motor neuron disorder. The neurotrophic factor, vascular endothelial growth factor, previously shown to be deficient in presymptomatic AR100 mice and which is linked to survival of motor neurons in both spinal and bulbar muscular atrophy (Sopher *et al*., 2004) and amyotrophic lateral sclerosis (Lambrechts *et al*., 2003; Azzouz *et al*., 2004; Storkebaum *et al*., 2005), and most recently to cerebellar neuron survival in spinocerebellar ataxia type 1 (SCA1, Cvetanovic *et al*., 2011), is regulated by the HIF1A transcription factor. HIF1A has been shown to interact with heat shock proteins (Isaacs *et al*., 2002; Huang *et al*., 2009). In this study, we show that administration of arimoclomol selectively upregulates the expression levels of Vegf both in the spinal cord and hindlimb muscles but interestingly not other genes linked with motor neuron and muscle perturbation in motor neuron disorders and polyglutamine diseases. It therefore suggests that arimoclomol may exert a neuroprotective effect by upregulation of the neurotrophic factor, vascular endothelial growth factor.

In conclusion, following a thorough physiological characterization of the decline in neuromuscular function in hindlimb muscles of AR100 mice, we established that long-term administration of arimoclomol is well tolerated without any appreciable side effects, and results in a significant amelioration in the disease phenotype of mice with spinal and bulbar muscular atrophy. The ability of arimoclomol to reduce the polyglutamine length-dependent neuromuscular phenotype as well as the motor neuronopathy observed in AR100 mice suggests that this co-inducer of the heat shock response may be of benefit in treating the pathology and symptoms underlying human spinal and bulbar muscular atrophy and potentially other neurodegenerative diseases.

Funding

This work was supported by the Institute of Neurology Kennedy's Disease Research Fund. The work was undertaken at University College London Hospitals/University College London, which received a proportion of funding from the Department of Health's National Institute for Health Research Biomedical

Research Centres funding scheme. N.N. was funded by an MRC Clinical Research Training Fellowship. The MRC Centre for Neuromuscular Diseases is supported by an MRC Centre grant G0601943. A.R.L. is supported by the NIH (R01 NS41648) and by a basic research grant from the Muscular Dystrophy Association. L.G. is the Graham Watts Senior Research Fellow, funded by The Brain Research Trust and the European Community's Seventh Framework Programme (FP7/2007-2013).

Supplementary material

Supplementary material is available at *Brain* online.

References

Abel A, Walcott J, Woods J, Duda J, Merry DE. Expression of expanded repeat androgen receptor produces neurologic disease in transgenic mice. Hum Mol Genet 2001; 10: 107–16.

Adachi H, Kume A, Li M, Nakagomi Y, Niwa H, Do J, et al. Transgenic mice with an expanded CAG repeat controlled by the human AR promoter show polyglutamine nuclear inclusions and neuronal dysfunction without neuronal cell death. Hum Mol Genet 2001; 10: 1039–48.

Adachi H, Katsuno M, Minamiyama M, Sang C, Pagoulatos G, Angelidis C, et al. Heat shock protein 70 chaperone overexpression ameliorates phenotypes of the spinal and bulbar muscular atrophy transgenic mouse model by reducing nuclear-localized mutant androgen receptor protein. J Neurosci 2003; 23: 2203–11.

Adachi H, Katsuno M, Minamiyama M, Waza M, Sang C, Nakagomi Y, et al. Widespread nuclear and cytoplasmic accumulation of mutant androgen receptor in SBMA patients. Brain 2005; 128: 659–70.

Adachi H, Waza M, Tokui K, Katsuno M, Minamiyama M, Tanaka F, et al. CHIP overexpression reduces mutant androgen receptor protein and ameliorates phenotypes of the spinal and bulbar muscular atrophy transgenic mouse model. J Neurosci 2007; 27: 5115–26.

Arrasate M, Mitra S, Schweitzer ES, Segal MR, Finkbeiner S. Inclusion body formation reduces levels of mutant huntingtin and the risk of neuronal death. Nature 2004; 431: 805–10.

Azzouz M, Ralph GS, Storkebaum E, Walmsley LE, Mitrophanous KA, Kingsman SM, et al. VEGF delivery with retrogradely transported lentivector prolongs survival in a mouse ALS model. Nature 2004; 429: 413–7.

Bailey CK, Andriola IF, Kampinga HH, Merry DE. Molecular chaperones enhance the degradation of expanded polyglutamine repeat androgen receptor in a cellular model of spinal and bulbar muscular atrophy. Hum Mol Genet 2002; 11: 515–23.

Banerji U, O'Donnell A, Scurr M, Pacey S, Stapleton S, Asad Y, et al. Phase I pharmacokinetic and pharmacodynamic study of 17-allylamino, 17-demethoxygeldanamycin in patients with advanced malignancies. J Clin Oncol 2005; 23: 4152–61.

Banno H, Katsuno M, Suzuki K, Tanaka F, Sobue G. Neuropathology and therapeutic intervention in spinal and bulbar muscular atrophy. Int J Mol Sci 2009; 10: 1000–12.

Bao XQ, Liu GT. Induction of overexpression of the 27- and 70-kDa heat shock proteins by bicyclol attenuates concanavalin A-induced liver injury through suppression of nuclear factor-kappaB in mice. Mol Pharmacol 2009; 75: 1180–88.

Bilsland LG, Dick JR, Pryce G, Petrosino S, Di Marzo V, Baker D, et al. Increasing cannabinoid levels by pharmacological and genetic manipulation delay disease progression in SOD1 mice. FASEB J 2006; 20: 1003–5.

Bowman AB, Yoo SY, Dantuma NP, Zoghbi HY. Neuronal dysfunction in a polyglutamine disease model occurs in the absence of ubiquitin-proteasome system impairment and inversely correlates with the degree of nuclear inclusion formation. Hum Mol Genet 2005; 14: 679–91.

Chahin N, Klein C, Mandrekar J, Sorenson E. Natural history of spinal-bulbar muscular atrophy. Neurology 2008; 70: 1967–71.

Chevalier-Larsen ES, O'Brien CJ, Wang H, Jenkins SC, Holder L, Lieberman A, et al. Castration restores function and neurofilament alterations of aged symptomatic males in a transgenic mouse model of spinal and bulbar muscular atrophy. J Neurosci 2004; 24: 4778–86.

Chomczynski P, Sacchi N. Single-step method of RNA isolation by acid guanidinium thiocyanate-phenol-chloroform extraction. Anal Biochem 1987; 162: 156–159.

Cowan KJ, Diamond MI, Welch WJ. Polyglutamine protein aggregation and toxicity are linked to the cellular stress response. Hum Mol Genet 2003; 12: 1377–91.

Crippa V, Sau D, Rusmini P, Boncoraglio A, Onesto E, Bolzoni E, et al. The small heat shock protein B8 (HspB8) promotes autophagic removal of misfolded proteins involved in amyotrophic lateral sclerosis (ALS). Hum Mol Genet 2010; 19: 3440–56.

Cudkowicz ME, Shefner JM, Simpson E, Grasso D, Yu H, Zhang H, et al. Arimoclomol at dosages up to 300 mg/day is well tolerated and safe in amyotrophic lateral sclerosis. Muscle Nerve 2008; 38: 837–44.

Cvetanovic M, Patel JM, Marti HH, Kini AR, Opal P. Vascular endothelial growth factor ameliorates the ataxic phenotype in a mouse model of spinocerebellar ataxia type 1. Nat Med 2011; 17: 1445–47.

Fischbeck KH. Kennedy disease. J Inherit Metab Dis 1997; 20: 152–8.

Fischbeck KH. Polyglutamine expansion neurodegenerative disease. Brain Res Bull 2001; 56: 161–3.

Fujikake N, Nagai Y, Popiel HA, Okamoto Y, Yamaguchi M, Toda T. Heat shock transcription factor 1-activating compounds suppress polyglutamine-induced neurodegeneration through induction of multiple molecular chaperones. J Biol Chem 2008; 283: 26188–97.

Gabai VL, Meriin AB, Mosser DD, Caron AW, Rits S, Shifrin VI, et al. Hsp70 prevents activation of stress kinases. A novel pathway of cellular thermotolerance. J Biol Chem 1997; 272: 18033–7.

Gatchel JR, Zoghbi HY. Diseases of unstable repeat expansion: mechanisms and common principles. Nat Rev Genet 2005; 6: 743–55.

Hands SL, Wyttenbach A. Neurotoxic protein oligomerisation associated with polyglutamine diseases. Acta Neuropathol 2010; 120: 419–37.

Hargitai J, Lewis H, Boros I, Rácz T, Fiser A, Kurucz I, et al. Bimoclomol, a heat shock protein co-inducer, acts by the prolonged activation of heat shock factor-1. Biochem Biophys Res Commun 2003; 307: 689–95.

Heinlein CA, Chang C. Role of chaperones in nuclear translocation and transactivation of steroid receptors. Endocrine 2001; 14: 143–9.

Huang WJ, Xia LM, Zhu F, Huang B, Zhou C, Zhu HF, et al. Transcriptional upregulation of HSP70-2 by HIF-1 in cancer cells in response to hypoxia. Int J Cancer 2009; 124: 298–305.

Isaacs JS, Jung YJ, Mimnaugh EG, Martinez A, Cuttitta F, Neckers LM. Hsp90 regulates a von Hippel Lindau-independent hypoxia-inducible factor-1 alpha-degradative pathway. J Biol Chem 2002; 277: 29936–44.

Kalmar B, Novoselov S, Gray A, Cheetham ME, Margulis B, Greensmith L. Late stage treatment with arimoclomol delays disease progression and prevents protein aggregation in the SOD1 mouse model of ALS. J Neurochem 2008; 107: 339–50.

Katsuno M, Adachi H, Kume A, Li M, Nakagomi Y, Niwa H, et al. Testosterone reduction prevents phenotypic expression in a transgenic mouse model of spinal and bulbar muscular atrophy. Neuron 2002; 35: 843–54.

Katsuno M, Adachi H, Tanaka F, Sobue G. Spinal and bulbar muscular atrophy: ligand-dependent pathogenesis and therapeutic perspectives. J Mol Med 2004; 82: 298–307.

Katsuno M, Sang C, Adachi H, Minamiyama M, Waza M, Tanaka F, et al. Pharmacological induction of heat-shock proteins alleviates polyglutamine-mediated motor neuron disease. Proc Natl Acad Sci U S A 2005; 102: 16801–6.

Katsuno M, Adachi H, Minamiyama M, Waza M, Tokui K, Banno H, et al. Reversible disruption of dynactin 1-mediated retrograde axonal

transport in polyglutamine-induced motor neuron degeneration. J Neurosci 2006; 26: 12106–17.

Katsuno M, Adachi H, Minamiyama M, Waza M, Doi H, Kondo N, et al. Disrupted transforming growth factor-beta signaling in spinal and bulbar muscular atrophy. J Neurosci 2010a; 30: 5702–12.

Katsuno M, Banno H, Suzuki K, Takeuchi Y, Kawashima M, Yabe I, et al. Efficacy and safety of leuprorelin in patients with spinal and bulbar muscular atrophy (JASMITT study): a multicentre, randomised, double-blind, placebo-controlled trial. Lancet Neurol 2010b; 9: 875–84.

Kieran D, Kalmar B, Dick JR, Riddoch-Contreras J, Burnstock G, Greensmith L. Treatment with arimoclomol, a coinducer of heat shock proteins, delays disease progression in ALS mice. Nat Med 2004; 10: 402–5.

Kobayashi Y, Kume A, Li M, Doyu M, Hata M, Ohtsuka K, et al. Chaperones Hsp70 and Hsp40 suppress aggregate formation and apoptosis in cultured neuronal cells expressing truncated androgen receptor protein with expanded polyglutamine tract. J Biol Chem 2000; 275: 8772–8.

La Spada AR, Wilson EM, Lubahn DB, Harding AE, Fischbeck KH. Androgen receptor gene mutations in X-linked spinal and bulbar muscular atrophy. Nature 1991; 352: 77–9.

Labbadia J, Cunliffe H, Weiss A, Katsyuba E, Sathasivam K, Seredenina T, et al. Altered chromatin architecture underlies progressive impairment of the heat shock response in mouse models of Huntington disease. J Clin Invest 2011; 121: 3306–19.

Lambrechts D, Storkebaum E, Morimoto M, Del-Favero J, Desmet F, Marklund SL, et al. VEGF is a modifier of amyotrophic lateral sclerosis in mice and humans and protects motoneurons against ischemic death. Nat Genet 2003; 34: 383–94.

Lanka V, Wieland S, Barber J, Cudkowicz M. Arimoclomol: a potential therapy under development for ALS. Expert Opin Investig Drugs 2009; 18: 1907–18.

Li M, Chevalier-Larsen ES, Merry DE, Diamond MI. Soluble androgen receptor oligomers underlie pathology in a mouse model of spinobulbar muscular atrophy. J Biol Chem 2007; 282: 3157–64.

Livak KJ, Schmittgen TD. Analysis of relative gene expression data using real-time quantitative PCR and the 2(-Delta Delta C(T)) Method. Methods 2001; 25: 402–408.

Malik B, Currais A, Andres A, Towlson C, Pitsi D, Nunes A, et al. Loss of neuronal cell cycle control as a mechanism of neurodegeneration in the presenilin-1 Alzheimer's disease brain. Cell Cycle 2008a; 7: 637–46.

Malik B, Currais A, Soriano S. Cell cycle-driven neuronal apoptosis specifically linked to amyloid peptide Abeta1-42 exposure is not exacerbated in a mouse model of presenilin-1 familial Alzheimer's disease. J Neurochem 2008b; 106: 912–6.

Malik B, Nirmalananthan N, Bilsland LG, La Spada AR, Hanna MG, Schiavo G, et al. Absence of disturbed axonal transport in spinal and bulbar muscular atrophy. Hum Mol Genet 2011; 20: 1776–86.

Malik B, Fernandes C, Killick R, Wroe R, Usardi A, Williamson R, et al. Oligomeric amyloid-beta peptide affects the expression of genes involved in steroid and lipid metabolism in primary neurons. Neurochem Int 2012; 61: 321–33.

Marfe G, Pucci B, De ML, Fiorito F, Di Stefano C, Indelicato M, et al. Heat-shock pretreatment inhibits sorbitol-induced apoptosis in K562, U937 and HeLa cells. Int J Cancer 2009; 125: 2077–85.

Montie HL, Cho MS, Holder L, Liu Y, Tsvetkov AS, Finkbeiner S, et al. Cytoplasmic retention of polyglutamine-expanded androgen receptor ameliorates disease via autophagy in a mouse model of spinal and bulbar muscular atrophy. Hum Mol Genet 2009; 18: 1937–50.

Muchowski PJ, Wacker JL. Modulation of neurodegeneration by molecular chaperones. Nat Rev Neurosci 2005; 6: 11–22.

Page TJ, Sikder D, Yang L, Pluta L, Wolfinger RD, Kodadek T, et al. Genome-wide analysis of human HSF1 signaling reveals a transcriptional program linked to cellular adaptation and survival. Mol Biosyst 2006; 2: 627–39.

Perutz MF, Johnson T, Suzuki M, Finch JT. Glutamine repeats as polar zippers: their possible role in inherited neurodegenerative diseases. Proc Natl Acad Sci U S A 1994; 91: 5355–8.

Pratt WB. The hsp90-based chaperone system: involvement in signal transduction from a variety of hormone and growth factor receptors. Proc Soc Exp Biol Med 1998; 217: 420–34.

Price JT, Quinn JM, Sims NA, Vieusseux J, Waldeck K, Docherty SE, et al. The heat shock protein 90 inhibitor, 17-allylamino-17-demethoxygeldanamycin, enhances osteoclast formation and potentiates bone metastasis of a human breast cancer cell line. Cancer Res 2005; 65: 4929–38.

Prudencio M, Durazo A, Whitelegge JP, Borchelt DR. An examination of wild-type SOD1 in modulating the toxicity and aggregation of ALS-associated mutant SOD1. Hum Mol Genet 2010; 19: 4774–89.

Qu M, Zhou Z, Xu S, Chen C, Yu Z, Wang D. Mortalin overexpression attenuates beta-amyloid-induced neurotoxicity in SH-SY5Y cells. Brain Res 2011; 1368: 336–45.

Ranganathan S, Fischbeck KH. Therapeutic approaches to spinal and bulbar muscular atrophy. Trends Pharmacol Sci 2010; 31: 523–27.

Rhodes LE, Freeman BK, Auh S, Kokkinis AD, La Pean A, Chen C, et al. Clinical features of spinal and bulbar muscular atrophy. Brain 2009; 132: 3242–51.

Ross CA. Polyglutamine pathogenesis: emergence of unifying mechanisms for Huntington's disease and related disorders. Neuron 2002; 35: 819–22.

Ross CA, Poirier MA. Protein aggregation and neurodegenerative disease. Nat Med 2004; 10 (Suppl): S10–17.

Ross CA, Poirier MA. Opinion: What is the role of protein aggregation in neurodegeneration? Nat Rev Mol Cell Biol 2005; 6: 891–8.

Ruchalski K, Mao H, Li Z, Wang Z, Gillers S, Wang Y, et al. Distinct hsp70 domains mediate apoptosis-inducing factor release and nuclear accumulation. J Biol Chem 2006; 281: 7873–80.

Rusmini P, Simonini F, Crippa V, Bolzoni E, Onesto E, Cagnin M, et al. 17-AAG increases autophagic removal of mutant androgen receptor in spinal and bulbar muscular atrophy. Neurobiol Dis 2011; 41: 83–95.

Sharp PS, Dick JR, Greensmith L. The effect of peripheral nerve injury on disease progression in the SOD1(G93A) mouse model of amyotrophic lateral sclerosis. Neuroscience 2005; 130: 897–910.

Simeoni S, Mancini MA, Stenoien DL, Marcelli M, Weigel NL, Zanisi M, et al. Motoneuronal cell death is not correlated with aggregate formation of androgen receptors containing an elongated polyglutamine tract. Hum Mol Genet 2000; 9: 133–44.

Sopher BL, Thomas PS Jr, LaFevre-Bernt MA, Holm IE, Wilke SA, Ware CB, et al. Androgen receptor YAC transgenic mice recapitulate SBMA motor neuronopathy and implicate VEGF164 in the motor neuron degeneration. Neuron 2004; 41: 687–99.

Stenoien DL, Cummings CJ, Adams HP, Mancini MG, Patel K, DeMartino GN, et al. Polyglutamine-expanded androgen receptors form aggregates that sequester heat shock proteins, proteasome components and SRC-1, and are suppressed by the HDJ-2 chaperone. Hum Mol Genet 1999; 8: 731–41.

Storkebaum E, Lambrechts D, Dewerchin M, Moreno-Murciano MP, Appelmans S, Oh H, et al. Treatment of motoneuron degeneration by intracerebroventricular delivery of VEGF in a rat model of ALS. Nat Neurosci 2005; 8: 85–92.

Suzuki K, Katsuno M, Banno H, Takeuchi Y, Atsuta N, Ito M, et al. CAG repeat size correlates to electrophysiological motor and sensory phenotypes in SBMA. Brain 2008; 131: 229–39.

Takahashi T, Kikuchi S, Katada S, Nagai Y, Nishizawa M, Onodera O. Soluble polyglutamine oligomers formed prior to inclusion body formation are cytotoxic. Hum Mol Genet 2008; 17: 345–56.

Takeyama K, Ito S, Yamamoto A, Tanimoto H, Furutani T, Kanuka H, et al. Androgen-dependent neurodegeneration by polyglutamine-expanded human androgen receptor in Drosophila. Neuron 2002; 35: 855–64.

Taylor JP, Tanaka F, Robitschek J, Sandoval CM, Taye A, Markovic-Plese S, et al. Aggresomes protect cells by enhancing the degradation of toxic polyglutamine-containing protein. Hum Mol Genet 2003; 12: 749–57.

Thomas PS Jr, Fraley GS, Damien V, Woodke LB, Zapata F, Sopher BL, et al. Loss of endogenous androgen receptor protein accelerates motor neuron degeneration and accentuates androgen insensitivity in a mouse model of X-linked spinal and bulbar muscular atrophy. Hum Mol Genet 2006; 15: 2225–38.

Tokui K, Adachi H, Waza M, Katsuno M, Minamiyama M, Doi H, et al. 17-DMAG ameliorates polyglutamine-mediated motor neuron degeneration through well-preserved proteasome function in an SBMA model mouse. Hum Mol Genet 2009; 18: 898–910.

Vandesompele J, De PK, Pattyn F, Poppe B, Van Roy N, De Paepe A, et al. Accurate normalization of real-time quantitative RT-PCR data by geometric averaging of multiple internal control genes. Genome Biol 2002; 3: RESEARCH0034.

Vigh L, Literati PN, Horvath I, Török Z, Balogh G, Glatz A, et al. Bimoclomol: a nontoxic, hydroxylamine derivative with stress protein-inducing activity and cytoprotective effects. Nat Med 1997; 3: 1150–54.

Walcott JL, Merry DE. Ligand promotes intranuclear inclusions in a novel cell model of spinal and bulbar muscular atrophy. J Biol Chem 2002; 277: 50855–9.

Watanabe M, Dykes-Hoberg M, Culotta VC, Price DL, Wong PC, Rothstein JD. Histological evidence of protein aggregation in mutant SOD1 transgenic mice and in amyotrophic lateral sclerosis neural tissues. Neurobiol Dis 2001; 8: 933–41.

Waza M, Adachi H, Katsuno M, Minamiyama M, Sang C, Tanaka F, et al. 17-AAG, an Hsp90 inhibitor, ameliorates polyglutamine-mediated motor neuron degeneration. Nat Med 2005; 11: 1088–95.

Williams AJ, Paulson HL. Polyglutamine neurodegeneration: protein misfolding revisited. Trends Neurosci 2008; 31: 521–8.

Wood JD, Beaujeux TP, Shaw PJ. Protein aggregation in motor neurone disorders. Neuropathol Appl Neurobiol 2003; 29: 529–45.

Wyttenbach A. Role of heat shock proteins during polyglutamine neurodegeneration: mechanisms and hypothesis. J Mol Neurosci 2004; 23: 69–96.

Yamagishi N, Goto K, Nakagawa S, Saito Y, Hatayama T. Hsp105 reduces the protein aggregation and cytotoxicity by expanded-polyglutamine proteins through the induction of Hsp70. Exp Cell Res 2010; 316: 2424–33.

Yoo SY, Pennesi ME, Weeber EJ, Xu B, Atkinson R, Chen S, et al. SCA7 knockin mice model human SCA7 and reveal gradual accumulation of mutant ataxin-7 in neurons and abnormalities in short-term plasticity. Neuron 2003; 37: 383–401.

Yu Z, Dadgar N, Albertelli M, Gruis K, Jordan C, Robins DM, et al. Androgen-dependent pathology demonstrates myopathic contribution to the Kennedy disease phenotype in a mouse knock-in model. J Clin Invest 2006; 116: 2663–72.